Journal of Alloys and Compounds 770 (2019) 229–235

Contents lists available at ScienceDirect

Journal of Alloys and Compounds

journal homepage: http://www.elsevier.com/locate/jalcom

High-pressure solid solutions of molecular hydrogen in amorphous magnesium silicates

Vadim S. Efimchenko*, Nikolay V. Barkovskii, Vladimir K. Fedotov, Konstantin P. Meletov, Sergey V. Simonov, Salavat S. Khasanov, Kirill I. Khryapin

Institute of Solid State Physics, Russian Academy of Sciences, Chernogolovka, Moscow District, 142432 Russia

ARTICLE INFO

Article history:
Received 30 March 2018
Received in revised form
27 July 2018
Accepted 13 August 2018
Available online 15 August 2018

Keywords:
Amorphous materials
Hydrogen absorbing materials
High-pressure
Raman spectroscopy

ABSTRACT

New amorphous solutions Mg_ySiO_{2+y}-XH_2 with the magnesium concentration varying from $y = 0$ to $y = 0.88$ were synthesized at a hydrogen pressure of 75 kbar and a temperature of 250 °C, followed by quenching to the temperature of liquid nitrogen. The quenched samples were studied by thermal desorption, X-ray diffraction and Raman spectroscopy. The X-ray diffraction study showed that all hydrogenated samples preserved the amorphous state and had no crystalline inclusions. At the same time, the positions of the first sharp diffraction peak (FSDP) of the samples with $y = 0.32$ and 0.6 were shifted by $\Delta Q = 0.14$ Å^{-1} after the hydrogenation thus signaling on changes in the amorphous network and even its small depolymerization.

According to the thermal desorption analysis, the hydrogen content X of the quenched Mg_ySiO_{2+y}-XH_2 samples nonlinearly decreased with increasing concentration y of the magnesium ions Mg^{2+} from $X = 0.600(3)$ at $y = 0$ to $X = 0.259(3)$ at $y = 0.88$. The samples with $y \geq 0.49$ evolved a significant portion of the dissolved hydrogen on heating in vacuum above 0 °C therefore showing a higher thermal stability than the hydrogenated silica and silicates with low magnesium concentrations. Raman spectroscopy demonstrated that hydrogen was dissolved in all samples in the form of H_2 molecules, and the width of the H_2 stretching line narrowed approximately four-fold with increasing magnesium concentration. Both this effect and the changes in the H_2 desorption kinetics presumably resulted from the decreasing dispersion in the size of silicate cavities in the amorphous matrix, which changes from the silica glass structure at $y \leq 0.32–0.49$ to the close-packed enstatite glass structure at higher magnesium concentrations.

1. Introduction

Among different types of hydrogenated substances, there is one that does not have a name yet. In the solid solutions and compounds of this type, hydrogen is present in the form of H_2 molecules, which are weakly bound to the host structures by Van der Waals forces. Earlier, the only representatives of hydrides of this type were hydrogen hydrates, such as the sII clathrate phase (5.6 wt % H_2) [1] and C_2 phase (10 wt % H_2) [2]. These hydrates were thoroughly investigated and the sII phase was even proposed as material for hydrogen storage [3].

Our recent studies revealed a considerable solubility of hydrogen in amorphous silica reaching 1.8 wt % H_2 (or a molar ratio H_2/f.u. of $X = 0.53$) at a hydrogen pressure of 75 kbar and a temperature of 250 °C [4]. Thus, the hydrogenated silica became the second example of concentrated solid solutions of molecular hydrogen.

Adding 0.6 mole of MgO to the silica network decreased the hydrogen solubility at $P = 75$ kbar in the amorphous silicate $Mg_{0.6}SiO_{2.6}$ to $X = 0.31$ [5]. On the other hand, the obtained amorphous compound $Mg_{0.6}SiO_{2.6}$-$0.31H_2$ showed a higher thermal stability in vacuum than SiO_2-$0.53H_2$ and evolved most of its hydrogen only after heating above 0 °C. Our studies by X-ray diffraction and Raman spectroscopy also showed [5] that the amorphous silicate network of the hydrogenated $Mg_{0.6}SiO_{2.6}$ undergoes a phase transition at 55 kbar, whereas the hydrogen dissolved in the amorphous silica prevents any changes in its structure at pressures up to 75 kbar [4]. Additionally, the stretching mode of H_2 molecules in the hydrogenated $Mg_{0.6}SiO_{2.6}$ samples proved to be

* Corresponding author.
E-mail address: efimchen@issp.ac.ru (V.S. Efimchenko).

https://doi.org/10.1016/j.jallcom.2018.08.111
0925-8388/

considerably narrowed both before and after the phase transition compared to that in the hydrogenated silica glass.

It seems worth mentioning here, too, that results of high-pressure high-temperature studies of the interaction of amorphous magnesium silicates with hydrogen could appear important for planetology and geophysics. For example, the magnesium silicates with Mg/Si from 0.7 to 2.4 in the amorphous form were found in the circumstellar dust of the evolved stars [6]. Such an amorphous dust compressed and heated by the gravitational forces together with hydrogen (the most abundant element of the Universe) could undergo the reactions playing a key role in the birth and first stages of evolution of planetary systems.

The present paper reports on the hydrogen content (X), network transformations, hydrogen state (atomic or molecular) and thermal stability of amorphous compounds Mg_ySiO_{2+y}-XH_2 with $y = 0–0.88$ loaded with hydrogen at $P = 75$ kbar and $T = 250$ °C. Each hydrogenated sample was rapidly cooled (quenched) from 250 °C to the N_2 boiling temperature and only warmed above this temperature when its hydrogen content was measured by hot extraction in vacuum. The quenched samples were studied by X-ray diffraction and Raman spectroscopy at ambient pressure and $T = -188$ °C.

2. Materials and methods

The silica glass was purchased from Sigma–Aldrich. Powders of the amorphous magnesium silicates were produced by a sol-gel method followed by sintering at 700 °C as described in Ref. [7]. According to results of the energy dispersive X-ray spectroscopy (EDX), the magnesium concentrations in the initial silicate samples Mg_ySiO_{2+y} thus produced were $y = 0$, 0.136, 0.32, 0.49, 0.6 and 0.88. These initial samples were examined by X-ray diffraction at room temperature on the Oxford diffraction equipment using Mo Kα radiation.

The hydrogenation of the silicates and silica glass was carried out in a Toroid-type high-pressure apparatus [8] using AlH_3 [9] or NH_3BH_3 [10] as an internal hydrogen source. The high-pressure cell was made of Teflon and the silicate and hydrogen source were separated by a Pd foil. To evolve hydrogen, AlH_3 or NH_3BH_3 was decomposed at $P = 15$ kbar by heating to $T = 250$ °C. The pressure was then increased and the silicate sample was exposed to an H_2 atmosphere at $P = 75$ kbar and $T = 250$ °C for 24 h and further rapidly cooled (quenched) to −196 °C to prevent hydrogen losses in the course of the subsequent pressure release. The molar ratio $X = H_2$/f.u. of the samples was determined with an accuracy of $\delta X = 0.03$ by hot extraction into a pre-evacuated volume [11].

The hydrogenated samples were stored in liquid nitrogen and further studied at ambient pressure by Raman spectroscopy at the liquid N_2 temperature and by X-ray diffraction at $T = -188$ °C. In view of the strong luminescence background from the powdered amorphous silica, we eventually switched to bulk samples of silica glass.

Raman spectra from the hydrogenated and initial samples were recorded in back-scattering geometry using a micro-Raman setup comprised of an Acton SpectraPro-2500i spectrograph and a CCD Pixis2K detector system cooled down to −70 °C. The measurements were performed near the liquid nitrogen temperature in the spectral range from 140 to 4500 cm^{-1}. The 532 nm line of a single-mode YAG CW diode pumped laser was focused on the sample by an Olympus 50 × objective in a ~2 μm diameter spot that was slightly defocused due to the light refraction in the nitrogen vapors. The spatial resolution was also ~2 μm and the spectral resolution varied between 2.3 and 4.1 cm^{-1}. The laser line was suppressed by a super-notch filter with the optical density $OD = 6$ and bandwidth ~160 cm^{-1}, while the beam intensity before the sample was ~5 mW.

The quenched samples were also studied by powder X-ray diffraction at ambient pressure and −188 °C using a Siemens D500 diffractometer equipped with a home-designed nitrogen cryostat that permitted loading metastable powder samples without their intermediate warming.

3. Results

The initial samples were shown to be amorphous and contain no crystalline inclusions. The positions, half-widths and integral intensities of the observed diffraction peaks are shown in Table 1. The obtained parameters vary from sample to sample, which indicates significant changes in the amorphous structure of the silicates caused by the varying Mg concentration. The first sharp diffraction peak (FSDP) gradually shifts from $Q = 1.58$ $Å^{-1}$ for pure SiO_2 to 1.89 $Å^{-1}$ for $Mg_{0.88}SiO_{2.88}$ due to the structural changes in the amorphous matrix of the samples with increasing magnesium concentration.

Fig. 1 depicts thermal desorption curves of the Mg_ySiO_{2+y}-XH_2 samples hydrogenated at $P = 75$ kbar. All samples start evolving hydrogen at a temperature near −187 °C. The pressure of the

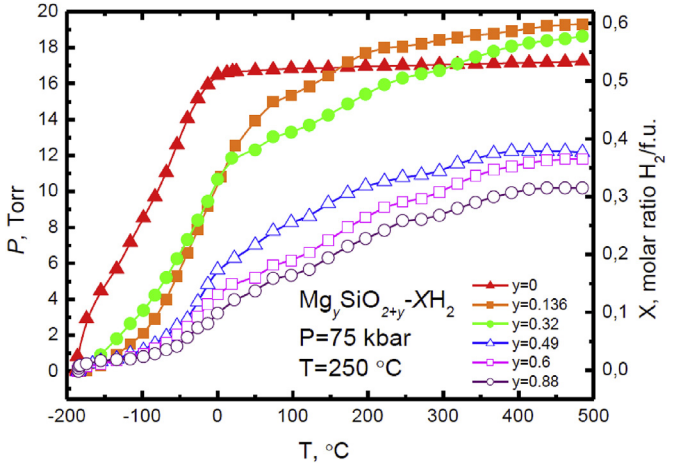

Fig. 1. Thermal desorption curves of the Mg_ySiO_{2+y}-XH_2 samples synthesized at $P = 75$ kbar and $T = 250$ °C and heated in vacuum at a rate of 20 °C/min. The curve for the hydrogenated amorphous silica ($y = 0$) is from Ref. [4].

Table 1
Positions (Q), half-widths ($\Delta_{½}$) and integral intensities (I) of peaks in the X-ray diffraction patterns of the initial Mg_ySiO_{2+y} samples. Room temperature, Mo Kα radiation.

Mg_ySiO_{2+y}	Q_1 $Å^{-1}$	$\Delta_{½}$ $Å^{-1}$	I_1 a.u.	Q_2 $Å^{-1}$	$\Delta_{½}$ $Å^{-1}$	I_2 a.u.	Q_3 $Å^{-1}$	$\Delta_{½}$ $Å^{-1}$
$y = 0$	1.579	0.510	1.40	4.920	1.416	0.124	6.55	–
$y = 0.136$	1.735	0.666	1.08	4.743	1.357	0.173	6.5	–
$y = 0.32$	1.832	0.811	0.84	4.620	1.417	0.181	6.4	–
$y = 0.49$	1.815	0.832	0.80	4.524	1.297	0.191	6.35	–
$y = 0.6$	1.869	0.905	0.75	4.360	1.296	0.170	6.2	0.76
$y = 0.88$	1.889	0.978	0.61	4.530	1.176	0.240	6.35	–

released gas gradually increases with increasing temperature within the whole studied interval of $T \leq 500\,^{\circ}C$. A few percent of the resulting pressure is however due to the evaporation of water and other gases condensed inside the quartz ampule in the course of loading the sample in the measuring system at the N_2 temperature. To eliminate this unwanted effect, the final value of the hydrogen content was calculated from the gas pressure remaining in the measuring system after condensing the impurity gases by cooling the ampoule with the sample to the liquid nitrogen temperature.

The shape of the desorption curves for the Mg_ySiO_{2+y}–XH_2 samples depends on the magnesium concentration (y). The curves for the samples with $y = 0.136$ and 0.32 look similar to the curve for SiO_2-H_2. Most of the hydrogen is released from these samples at temperatures below 0 °C. In contrast, the Mg_ySiO_{2+y}-H samples with higher magnesium concentrations $y = 0.49$, 0.6 and 0.88 release most their hydrogen at temperatures well above 0 °C.

The total amount of hydrogen released from each Mg_ySiO_{2+y}-XH_2 sample heated in vacuum to 500 °C is presented in Fig. 2 as a function of the magnesium concentration *y*. The horizontal error bars indicate the inaccuracy in determining the magnesium concentrations by EDX.

As seen from Fig. 2, the hydrogen content of the bulk sample of silica glass ($X = 0.60$) is higher than that of the powder one ($X = 0.53$). Most likely, this is because the concentration of the larger interstitial voids accessible for hydrogen is higher in the bulk silica glass produced by quenching from the melt than in the powder of amorphous silica produced by the sol-gel method. Such an assumption agrees with results of earlier Raman studies [12], which established different type distributions of the Si-O-Si rings in the samples of amorphous silica produced by the above methods.

As one can also see from Fig. 2, the X(y) dependence for the Mg_ySiO_{2+y}-XH_2 samples steeply decreases in the concentration interval $0.32 < y < 0.49$. Our further studies of the quenched samples by Raman spectroscopy showed that the amorphous states of the Mg_ySiO_{2+y}-XH_2 silicates with $y \leq 0.32$ and $y \geq 0.49$ were significantly different.

According to [4], the incorporation of hydrogen molecules into the amorphous network of SiO_2 reduced its compressibility and prevented the collapse of the voids at pressures up to 75 kbar. This effect manifested itself in the absence of any detectable shift of the first sharp diffraction peak FSDP in the X-ray spectra of a sample of silica glass after its hydrogenation at high pressures. In contrast, hydrogenation of amorphous $Mg_{0.6}SiO_{2.6}$ at hydrogen pressures above 55 kbar resulted in a considerable shift of its FSDP from 1.84 A to 2 $Å^{-1}$, and this shift was mostly caused by an irreversible densification of the silicate. A similar shift of FSDP was also observed for the amorphous $Mg_{0.6}SiO_{2.6}$ compound pressurized in Teflon without hydrogen.

The present X-ray diffraction study (Fig. 3) showed that the FSDP in the structure factor S(Q) of the quenched $Mg_{0.32}SiO_{2.32}$-$0.5H_2$ sample is also shifted by $\Delta Q = 0.14$ $Å^{-1}$ relative to its position in the initial compound. The shift is approximately the same as in the hydrogenated $Mg_{0.6}SiO_{2.6}$ compound [5], while the hydrogen content of $Mg_{0.32}SiO_{2.32}$-$0.5H_2$ is close to that of the hydrogenated amorphous silica, which demonstrated no shift [4].

The incorporation of magnesium cations is known to lead to destruction of the Si-O-Si chemical bonds, thus depolymerizing the three-dimensional silica network and changing its elastic moduli. We therefore expect that even a small addition of magnesium cations should noticeably reduce the stability of silica glass under pressure and outweigh the effect of dissolved hydrogen on the compressibility of the silica network.

The influence of depolymertization of the silica network on the dissolved hydrogen was studied by Raman spectroscopy. Fig. 4 shows the collected Raman spectra of the hydrogenated silicates Mg_ySiO_{2+y}-XH_2 measured at frequencies from 200 to 4400 cm^{-1} at ambient pressure on the samples submerged in liquid nitrogen.

The increase in the magnesium concentration reduces the intensities of the wide band at 350–500 cm^{-1} and a band at 800 cm^{-1}. In contrast, the intensity of the band at 800–1200 cm^{-1} strongly increases in the samples with high magnesium concentrations $y \geq 0.49$. None of the spectra shows noticeable Raman intensity in the frequency range 1200–1400 cm^{-1}, where an unidentified vibrational band was earlier observed in the spectrum of amorphous $Mg_{0.6}SiO_{2.6}$-$0.31H_2$ [5]. Presumably, that band could result from the boron nitride condensed on the surface of the hydrogenated sample after decomposing NH_3BH_3 [13] used as the

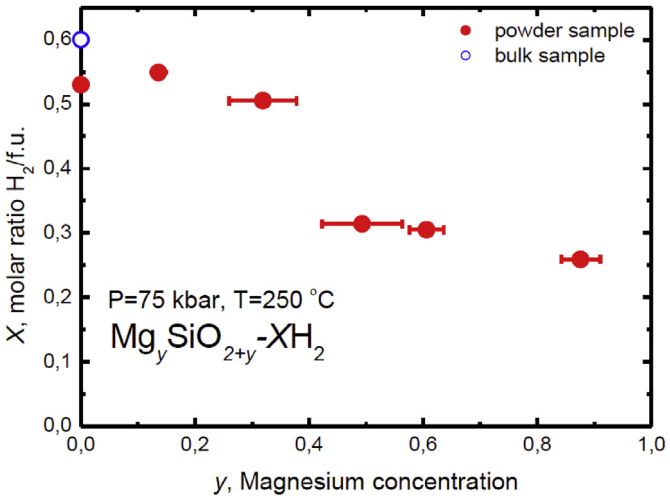

Fig. 2. The total hydrogen content X of the Mg_ySiO_{2+y}-XH_2 samples as a function of the magnesium concentration *y*. The open blue circle shows the hydrogen content of the bulk silica glass. The solid red circles stand for the hydrogen contents of the powder samples. The data for the powder sample of hydrogenated amorphous silica ($y = 0$) is taken from Ref. [4]. The horizontal error bars shows the inaccuracy in the magnesium concentrations determined by EDX. (For interpretation of the references to colour in this figure legend, the reader is referred to the Web version of this article.)

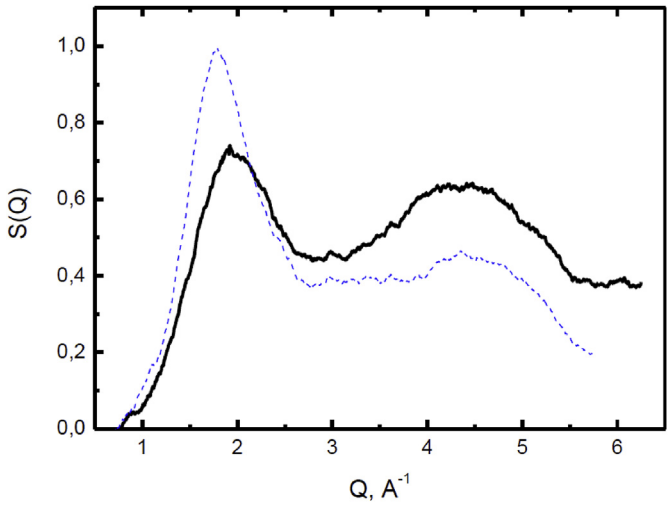

Fig. 3. Structure factors S(Q) for the amorphous silicate $Mg_{0.32}SiO_{2.32}$ before (dashed blue line) and after (solid black line) its hydrogenation to $X = 0.5$ at 75 kbar and 250 °C. The presented X-ray data were collected at ambient pressure and $T = -188\,^{\circ}C$ using Cu Kα radiation. (For interpretation of the references to colour in this figure legend, the reader is referred to the Web version of this article.)

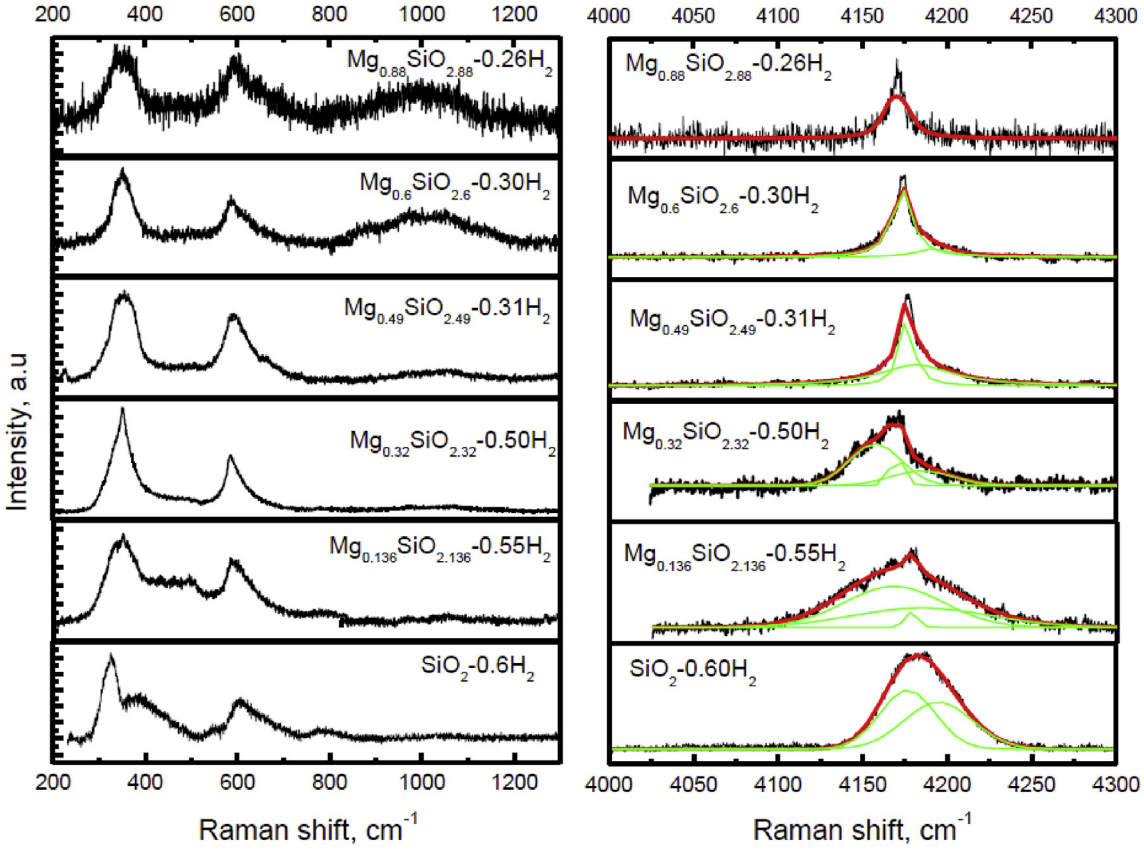

Fig. 4. Raman spectra for the Mg_ySiO_{2+y}-XH_2 samples loaded with hydrogen under a hydrogen pressure of 75 kbar and T = 250 °C. The black thick lines represent the experimental spectra collected at T = −196 °C and ambient pressure. The thin green lines show the peaks produced by decomposition of the H-H stretching bands into Gaussians or Lorentzians. The thick red lines embody the resulting groups of Gaussians or Lorentzians. (For interpretation of the references to colour in this figure legend, the reader is referred to the Web version of this article.)

hydrogen source in Ref. 5.

The presence of a band in the frequency range 4150–4250 cm^{-1} (right panel of Fig. 4) characteristic of stretching H-H vibrations shows that hydrogen was dissolved in the form of H_2 molecules in all investigated samples. The measured Raman spectra also include rotational lines of the H_2 molecules at 326 and 597 cm^{-1} in the hydrogenated silica glass and at 348 and 586 cm^{-1} in the magnesium silicates (left panel of Fig. 4).

As seen from Fig. 4, the stretching H-H band of the SiO_2-H_2 sample can be well approximated by two wide Gaussian peaks. The bands from the magnesium-containing samples have a more complicated shape and obviously contain a few lines with different frequencies and widths. The green lines in Fig. 4 show the Lorentz or Gaussian peaks obtained by decomposition of the H-H stretching bands. The bands in the spectra of the samples with y = 0.136 and 0.32 were decomposed into Gaussians as those for the silica glass. In the case of the samples with y ≥ 0.49, the Lorentzian expansion was more appropriate. The H-H stretching peak of the sample with the highest magnesium concentration y = 0.88 could not be accurately fitted by any combination of Gaussians or Lorentzians and we approximated it by one Lorentz dominating line at 4169 cm^{-1}.

Fig. 5 shows relative intensities vs. frequencies for the Lorentzians and Gaussians obtained by fitting the experimental H-H stretching lines. The Lorentzians and Gaussians can roughly be divided into two groups: wide peaks with the average width $\Delta = 44 \pm 15$ cm^{-1} and narrow peaks with $\Delta = 10 \pm 2$ cm^{-1}. As seen from Fig. 5, the frequencies of the wide peaks significantly change with increasing magnesium concentration, while their intensities

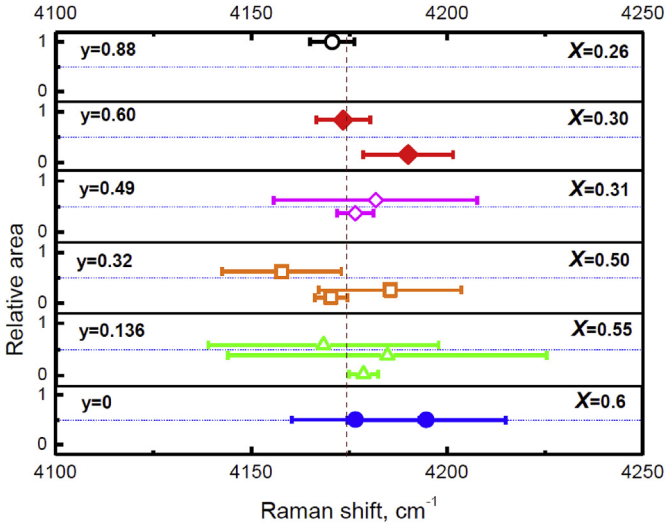

Fig. 5. Relative integral intensities of the Lorentzians and Gaussians resulting from the decomposition of the H_2 stretching bands in the Raman spectra of the quenched Mg_ySiO_{2+y}-XH_2 samples. The symbols indicate the frequencies and relative areas (integral intensities) of the Lorentzians and Gaussians. The horizontal bars show the full width at half peak (FWHP) of the corresponding Lorentzians and Gaussians. The vertical dashed line indicates the average frequency of the narrow peaks (see text).

gradually decrease until these peaks nearly vanish at y = 0.88. The narrow peaks are absent in the Raman spectra of hydrogenated

silica glass. They appear at 4169 and 4178 cm^{-1} in the spectrum of the hydrogenated silicate with the minimal Mg concentration y = 0.136 (see right panel of Fig. 4) and their positions nearly do not change in the spectra of the silicates with higher y. The average frequency 4174 $cm^{-1}$of these peaks is shown by the vertical dashed line in Fig. 5.

The sums of the relative intensities of the wide and, separately, of the narrow peaks are shown in Fig. 6 as functions of the magnesium concentration in the hydrogenated silicates. As seen in Fig. 6, the integral intensities of the wide peaks gradually decrease with increasing Mg concentration, while the integral intensities of the narrow peaks increase, so that only one narrow peak remains at 4169 cm^{-1} in the spectrum of the sample with the maximal y = 0.88.

It is worth noting that these effects are concomitant with the gradual disappearance of the band of bending vibrations of the SiO_2 network at 300–500 cm^{-1} and rising intensity of the Si-O-Si stretching band at 800–1200 cm^{-1}. According to the literature data [7], cations of alkaline earth elements incorporated into the silica network depolymerize it by breaking or weakening oxygen bridges between the SiO_4 tetrahedrons. The resulting inhomogeneous framework contains both isolated SiO_4 clusters and clusters partly linked by one, two, three or four oxygen atoms. Correspondingly, the Raman stretching band of the Mg_ySiO_{2+y} amorphous compounds is wide and includes frequencies from 850 cm^{-1} for the isolated SiO_4 tetrahedrons (Mg_2SiO_4 glass) to 1200 cm^{-1} for the continuous SiO_4 network (pure silica glass) [14].

4. Discussion

The amorphous network of the silica glass is known to consist of different types of voids accessible for hydrogen molecules [15]. Earlier Raman investigations performed on the silica glass samples with low hydrogen concentrations (X = 0.03) showed that the interaction of the H_2 molecules with the silica "walls" of interstices leads to the appearance of one broad Lorentz stretching band at 4142 ± 2 cm^{-1} with the width Δ ~ 25 cm^{-1} [16]. Using the width of this band, the size of H_2 molecules and their thermal velocity, the authors of [16] made an estimate of 7 Å for the average dimensions of the voids occupied by hydrogen.

The stretching band of the SiO_2-XH_2 sample with X = 0.6 measured in the present work (see Fig. 5) is well approximated by two Gauss peaks with the frequencies 4176 and 4195 cm^{-1} and widths Δ = 32.5 and 40.4 cm^{-1}, respectively. The increase of these widths in comparison with Δ ~25 cm^{-1} for the SiO_2-XH_2 sample with a much lower X = 0.03 studied earlier [16] is likely to be due to the penetration of hydrogen molecules into new types of voids with different H_2-SiO_2 interaction. In view of the high hydrogen content of our sample, broadening of its vibrational bands due to the interaction between hydrogen molecules cannot be excluded either because of the possible multiple occupancy of some voids by two or more closely located H_2 molecules. Multiple occupancy of large voids by H_2 molecules was earlier observed in the sII clathrate structure of hydrogen hydrates [1].

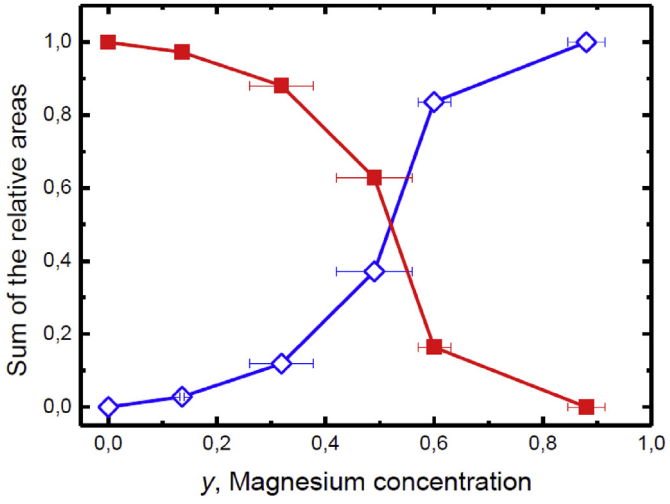

Fig. 6. Sums of the integral intensities of the narrow (open diamonds) and wide (solid squares) decomposed H-H lines vs. the magnesium concentration in the Mg_ySiO_{2+y}-XH_2 samples.

We can think of two possible explanations of the abrupt narrowing of the H-H stretching band at the magnesium concentrations exceeding y > 0.32 in the Mg_ySiO_{2+y}-XH_2 samples. One possibility is that a considerable part of the dissolved hydrogen formed strong chemical bonds with the host network, so that only vibrations of the H_2 molecules occupying large voids and loosely bound to the matrix could form the H-H stretching band. However, the Raman spectra showed no bands of the Si-H, Si-OH or Mg-OH stretching vibrations in the corresponding frequency regions. This suggests that the concentrations of these species in the quenched samples were below the detection limit of 2–3 mol. % of the spectroscopic technique used.

Another and a more likely explanation can be deduced from the fact that the abrupt narrowing of the H_2 stretching band is accompanied by the abrupt decrease in the hydrogen content of the Mg_ySiO_{2+y}-XH_2 samples from X ~0.5 at y ≤ 0.32 to X ~0.3 at y ≥ 0.49 (see Fig. 2). This signals on strong qualitative changes in the amorphous network of the initial Mg_ySiO_{2+y} samples in the concentration interval 0.32 ≤ y ≤ 0.49.

It is known [17] that silica glass has voids constructed of 3–12 membered Si-O-Si rings. The distribution of the rings over different fractions has a maximum for the 6-membered rings. In contrast, the amorphous network of the enstatite glass $MgSiO_3$ has only voids constructed by two, three, four, five and small amount of six-membered Si(Mg)-O-Si(Mg) rings [17]. The distribution of the rings in $MgSiO_3$ is much narrower than in silica glass and has a maximum at the 4-membered rings. The voids constructed of the 3- or less-membered rings are inaccessible for hydrogen because their diameter is smaller than that of the H_2 molecule (2.5 Å) [15]. Consequently, only voids formed by the 4, 5 and 6-membered rings are accessible for H_2 molecules in the structure of $MgSiO_3$. Such a limitation should reduce the hydrogen solubility and lead to a smaller width of the H-H stretching band in the Raman spectrum of this compound because the interaction of hydrogen molecules with the walls of interstices in $MgSiO_3$ should be less variable than in the silica glass.

Additionally, the small volume of the most abundant voids formed by the 4-membered rings in $MgSiO_3$ does not allow them to accommodate more than one H_2 molecule. This kills the H_2-H_2 interaction because the interaction between the hydrogen molecules located in different voids is effectively screened by the silicate neighborhood. As a result, the width of the H-H stretching band is further reduced.

The steep increase in the integral intensity of the narrow H-H stretching peak at y > 0.32 (see Fig. 7) also points to qualitative changes in the amorphous network of the Mg_ySiO_{2+y} compounds. To show this, consider a simple model of amorphous hydrogen solutions Mg_ySiO_{2+y}-XH_2 consisting of clusters of the two limiting compounds, $SiO_2H_{1.2}$ and $Mg_{0.88}SiO_{2.88}H_{0.52}$. Among the silicates studied in the present work, $Mg_{0.88}SiO_{2.88}$ has the composition closest to the enstatite glass and should therefore have a similar voids distribution. Assuming the intensity *I* of the narrow peak to be proportional to the total amount of H_2 molecules in the

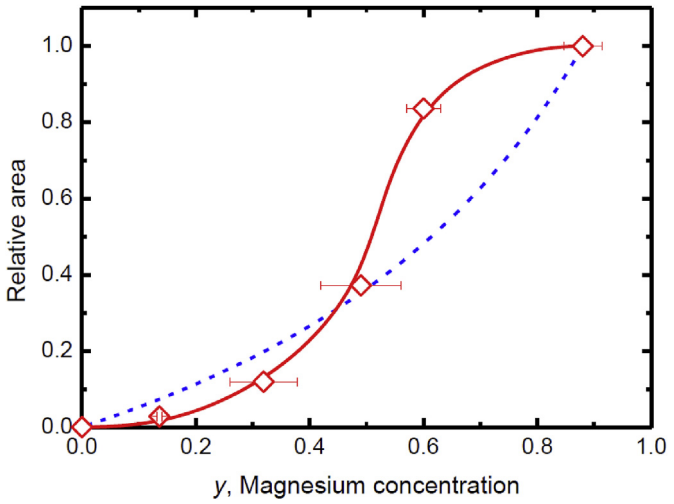

Fig. 7. The experimental (symbols) and calculated (dashed line) relative integral intensities of the narrow H-H stretching lines vs. the magnesium concentration in the Mg_ySiO_{2+y}-XH_2 samples. The thick solid line is a guide for the eyes. The horizontal error bars shows the inaccuracy in the magnesium concentrations. The inaccuracy in the relative integral intensity of the narrow peaks is less than the symbol size.

enstatite-like $Mg_{0.88}SiO_{2.88}H_{0.52}$ clusters, this gives:

$$I(y) = \left[1 + \frac{X_s}{X_e} \cdot \frac{1 - Y_e}{Y_e}\right]^{-1}, \quad (1)$$

where $X_s = 0.6$ and $X_e = 0.26$ are the hydrogen contents of the silica-like and enstatite-like clusters; $Y_e = y/0.88$ is the concentration of the enstatite-like clusters.

Dependence (1) is shown in Fig. 7 by the dashed line. The calculated curve satisfactorily agrees with experiment at $y \leq 0.49$. The negative difference between the calculated and experimental values can easily be explained under the assumption that the formation of the $Mg_{0.88}SiO_{2.88}H_{0.52}$ clusters is accompanied by an increase in the concentration of magnesium cations in the silica glass network. The latter decreases the number of the enstatite-like clusters and does not induce significant structural changes in the silica matrix, because at low concentrations, the cations predominantly occupy large voids in it and sit on the positions most distant from the oxygen atoms [17].

However, at $y > 0.32$, the experimental I(y) values begin to rapidly increase, so that the I(0.6) point appears much above the calculated curve. Such a steep increase in the intensity of the narrow peak could only occur if the amorphous structure of the samples as a whole undergoes a transition to the enstatite-like structure at $0.32 < y < 06$. Such a transition also explains the steep decrease of the hydrogen solubility in amorphous Mg_ySiO_{2+y} silicates from X ~0.5 at $y \leq 0.32$ to X ~0.3 at $y \geq 0.49$ (Fig. 2).

Thus, both Raman spectroscopy and hydrogen solubility measurements demonstrate that the Mg_ySiO_{2+y}-XH_2 amorphous compounds with the low ($y \leq 0.32$) and high ($y \geq 0.49$) magnesium concentrations have significantly different structures, which are similar to the initial structures of the silica glass and enstatite glass, respectively. The different thermal stability of the hydrogenated silicates with $y \leq 0.32$ and $y \geq 0.49$ (see Fig. 1) also corroborates the conclusion about the qualitatively different structures of these two groups of amorphous silicates.

5. Conclusions

New amorphous solid solutions Mg_ySiO_{2+y}-XH_2 with $y = 0–0.88$ are synthesized at a hydrogen pressure of 75 kbar and studied by thermal desorption, X-ray diffraction and Raman spectroscopy. The hydrogen content of the hydrogenated powder samples decreases from $X = 0.60$ at $y = 0$ (pure SiO_2 glass) to $X = 0.26$ at $y = 0.88$. The decrease in the X(y) dependence is most steep in the interval $0.32 < y < 0.49$ that divides the samples into two groups, which have lower and higher magnesium concentrations and differ from each other by thermal stability and Raman spectra. The behaviors of the samples with $y \leq 0.32$ are similar to those of the H_2 solid solutions in pure silica glass. The samples with $y \geq 0.49$ all behave similar to the solid solutions with the maximal magnesium concentration $y = 0.88$. As discussed in the paper, the differences in the properties of the two groups of hydrogenated silicates could be attributed to the different structures of the initial amorphous compounds Mg_ySiO_{2+y}. Namely, the compounds with $y \leq 0.32$ are similar to silica glass, whereas the compounds with $y \geq 0.49$ have structures characteristic of the enstatite glass $MgSiO_3$.

A common property of the solid solutions Mg_ySiO_{2+y}-XH_2 with $y \geq 0.32$ is their irreversible densification at a hydrogen pressure of 75 kbar and $T = 250\,^{\circ}C$. This distinguishes magnesium silicates from pure silica glass, which is irreversibly compacted under these pressure and temperature if compressed in a large-molecule medium [18], but experiences no irreversible structural changes in a hydrogen atmosphere [4]. Most likely, this is a partial depolymerization of the silica glass structure caused by the dissolved magnesium cations, which makes the structure of the silicates and their hydrides less resistant to pressure.

Acknowledgement

The work was supported by grant No. 15-02-08508 from the Russian Foundation for Basic Research and by the Program “Physics of Fundamental Interactions and Nuclear Technologies” of the Russian Academy of Sciences.

References

[1] W.L. Mao, H.-K. Mao, A.F. Goncharov, V.V. Struzhkin, Q. Guo, J. Hu, J. Shu, R.J. Hemley, M. Somayazulu, Y. Zhao, Hydrogen clusters in clathrate hydrate, Science 297 (2002) 2247–2249. https://doi.org/10.1126/science.1075394.
[2] W. Vos, L. Finger, R. Hemley, H.-K. Mao, Novel H_2–H_2O clathrates at high pressures, Phys. Rev. Lett. 71 (1993) 3150–3153. https://doi.org/10.1103/PhysRevLett.71.3150.
[3] W.L. Mao, H.-K. Mao, Hydrogen storage in molecular compounds, Proc. Natl. Acad. Sci. U.S.A. 101 (2004) 708–710. https://doi.org/10.1073/pnas.0307449100.
[4] V.S. Efimchenko, V.K. Fedotov, M.A. Kuzovnikov, A.S. Zhuravlev, B.M. Bulychev, Hydrogen solubility in amorphous silica at pressures up to 75 kbar, J. Phys. Chem. B 117 (2013) 422–425, https://doi.org/10.1021/jp309991x.
[5] V.S. Efimchenko, N.V. Barkovskii, V.K. Fedotov, K.P. Meletov, Hydrogen solubility in amorphous $Mg_{0.6}SiO_{2.6}$ at high pressure, J. Exp. Theor. Phys. 124 (2017) 914–919. https://doi.org/10.1134/S1063776117050028.
[6] C. Jäger, J. Dorschner, H. Mutschke, T. Posch, T. Hennin, Steps toward interstellar silicate mineralogy VII. Spectral properties and crystallization behaviour of magnesium silicates produced by the sol-gel method, Astron. Astrophys. 408 (2003) 193–204. https://doi.org/10.1051/0004-6361:20030916.
[7] A.G. Kalampounias, IR and Raman spectroscopic studies of sol–gel derived alkaline-earth silicate glasses, Bull. Mater. Sci. 34 (2011) 299–303. https://doi.org/10.1007/s12034-011-0064-x.
[8] L.G. Khvostantsev, V.N. Slesarev, V.V. Brazhkin, Toroid type high-pressure device: history and prospects, High Press. Res. 24 (2004) 371–383. https://doi.org/10.1080/08957950412331298761.
[9] V.E. Antonov, I.O. Bashkin, S.S. Khasanov, A.P. Moravsky, Yu.G. Morozov, Yu.M. Shulga, Yu.A. Ossipyan, E.G. Ponyatovsky, Magnetic ordering in hydrofullerite $C_{60}H_{24}$, J. Alloys Compd. 330–332 (2002) 365–368. https://doi.org/10.1016/S0925-8388(01)01534-1.
[10] V.E. Antonov, B.M. Bulychev, V.K. Fedotov, et al., NH_3BH_3 as an internal hydrogen source for high pressure experiments, Int. J. Hydrogen Energy 42 (2017) 22454–22459. https://doi.org/10.1016/j.ijhydene.2017.03.121.
[11] I.O. Bashkin, V.E. Antonov, A.V. Bazhenov, et al., Thermally stable hydrogen compounds obtained under high pressure on the basis of carbon nanotubes and nanofibers, JETP Lett. 79 (2004) 226–230. https://doi.org/10.1134/1.

1753421.
[12] A. Chrissanthopoulos, N. Bouropoulos, S.N. Yannopoulos, Vibrational spectroscopic and computational studies of sol–gel derived CaO–MgO–SiO2 binary and ternary bioactive glasses, Vib. Spectrosc. 48 (2008) 118–125. https://doi.org/10.1016/j.vibspec.2007.11.008.
[13] J. Nylén, T. Sato, E. Soignard, J.L. Yarger, E. Stoyanov, U. Häussermann, Thermal decomposition of ammonia borane at high pressures, J. Chem. Phys. 131 (2009) 104506–104513. https://doi.org/10.1063/1.3230973.
[14] P. McMillan, Structural studies of silicate glasses and melts-applications and limitations of Raman spectroscopy, Am. Mineral. 69 (1984) 622.
[15] R.J. Bell, P. Dean, The structure of vitreous silica: validity of the random network theory, Philos. Mag. 25 (1972) 1381–1398. https://doi.org/10.1080/14786437208223861.
[16] C.M. Hartwig, Raman scattering from hydrogen and deuterium dissolved in silica as a function of pressure, J. Appl. Phys. 47 (1976) 956–959. https://doi.org/10.1063/1.322686.
[17] S. Kohara, J. Akola, H. Morita, et al., Relationship between topological order and glass forming ability in densely packed enstatite and forsterite composition glasses, Proc. Natl. Acad. Sci. 108 (2011) 14780–14785. https://doi.org/10.1073/pnas.1104692108.
[18] Y. Inamura, Y. Katayama, W. Utsumi, K. Funakoshi, Transformations in the intermediate-range structure of SiO_2 glass under high pressure and temperature, Phys. Rev. Lett. 93 (2004) 015501–015504. https://doi.org/10.1103/PhysRevLett.93.015501.